

000 001 002 003 004 005 006 007 008 009 010 011 012 013 014 015 016 017 018 019 020 021 022 023 024 025 026 027 028 029 030 031 032 033 034 035 036 037 038 039 040 041 042 043 044 045 046 047 048 049 050 051 052 053 MEDIX-R1: OPEN ENDED MEDICAL REINFORCE- MENT LEARNING

Anonymous authors

Paper under double-blind review

ABSTRACT

We introduce MediX-R1, an open-ended reinforcement learning (RL) framework for medical multimodal large language models (MLLMs) that enables clinically grounded, free-form answers beyond multiple-choice formats. MediX-R1 fine-tunes a baseline vision–language backbone with Group Relative Policy Optimization (GRPO) and a composite reward tailored for medical reasoning: an LLM-based accuracy reward that judges semantic correctness with a strict YES/NO decision, a medical embedding-based semantic reward to capture paraphrases and terminology variants, and lightweight format and modality rewards that enforce interpretable reasoning and modality recognition. This multi-signal design provides stable, informative feedback for open-ended outputs where traditional verifiable or MCQ-only rewards fall short. To measure progress, we propose a unified evaluation framework for both text-only and image+text tasks that uses an LLM-as-judge in place of brittle string-overlap metrics, capturing semantic correctness, reasoning, and contextual alignment. Despite using only $\sim 50K$ instruction examples, MediX-R1 achieves excellent results across standard medical LLM and VLM benchmarks, outperforming strong open-source baselines and delivering particularly large gains on open-ended clinical tasks (e.g., radiology summarization and report generation). Our results demonstrate that open-ended RL with comprehensive reward signals and LLM-based evaluation is a practical path toward reliable medical reasoning in multimodal models. Our trained models, curated datasets and source code will be publicly released.

1 INTRODUCTION

Large medical language and vision–language models are increasingly deployed for clinical question answering, triage support, report drafting, and education (Chen et al., 2024a; Sellergren et al., 2025; Pieri et al., 2024). Many of these tasks are inherently open-ended: clinicians expect concise but free-form answers that can flexibly incorporate context, uncertainty, and multimodal evidence. However, most training and evaluation pipelines remain tailored to Multiple Choice Questions (MCQ) or string-matching regimes, which (i) under-reward valid clinical paraphrases, (ii) fail to measure reasoning quality or modality recognition, and (iii) do not provide reliable signals for reinforcement learning (RL) in open-ended settings. As a result, models trained only with supervised objectives or MCQ-style rewards often struggle to produce faithful, interpretable, and robust clinical responses across diverse modalities.

RL has improved reasoning in domains with verifiable rewards (e.g., math and code) as shown by DeepSeek models (Shao et al., 2024; Guo et al., 2025), but medical tasks rarely admit executable checks. Binary exact match is too brittle for clinical phrasing; BLEU/ROUGE can mis-score semantically correct answers; and free-form VLM outputs complicate visual inference. Moreover, using a single reward signal can induce instability or reward hacking, especially when the signal is noisy (LLM-as-judge) or overly permissive (embedding similarity). Hence, it is desirable to have a principled approach for training medical MLLMs with open-ended RL that integrates semantic correctness with structural and modality constraints, while remaining data- and compute-efficient.

We present MediX-R1, an open-ended medical RL framework that fine-tunes a baseline multimodal backbone with Group Relative Policy Optimization (GRPO) (Shao et al., 2024) using a composite reward tailored for clinical reasoning. Our design combines: (1) an LLM-based accuracy reward that

Model	Diverse Medical Modalities	Single-Stage RL	Interpretable Reasoning	Open-Ended Responses	Annotation-Free Reasoning	Composite RL Reward
MedVLM-R1	✗	✓	✓	✗	✓	✗
BiMediX2	✓	✗	✗	✓	✗	✗
HuatuoGPT-V	✓	✗	✗	✓	✗	✗
MedGemma	✓	✗	✓	✓	✗	✗
MediX-R1	✓	✓	✓	✓	✓	✓

Table 1: **Model capability comparison.** MediX-R1 integrates diverse modalities, interpretable reasoning, and composite RL rewards, enabling practical clinical use.

enforces a strict YES/NO decision on semantic correctness, (2) a medical embedding-based semantic reward that captures paraphrases and terminology variants, (3) a lightweight format reward that elicits interpretable reasoning traces, and (4) a modality recognition reward that discourages cross-modality hallucinations by requiring explicit modality tags. This multi-signal objective stabilizes optimization and supplies informative feedback where traditional verifiable or MCQ-only rewards fall short, enabling single-stage, open-ended RL directly on clinical tasks.

Table 1 contrasts MediX-R1 with strong open models across key clinical capabilities. First, on *Diverse Medical Modalities*, MediX-R1 supports diverse medical modalities including X-Ray, CT, MRI, Microscopy/Histopathology, Ultrasound, Fluoroscopy, Endoscopy, Angiography, Mammography, Clinical Photography, SPECT (Single Photon Emission Computed Tomography), OCT (Optical Coherence Tomography), and Fundus imaging, whereas MedVLM-R1 (Pan et al., 2025) is limited to radiology images. Models like MedGemma (Sellergren et al., 2025), HuatuoGPT-Vision (Chen et al., 2024b), and BiMediX2 (Mullappilly et al., 2024) provide coverage on clinical modalities but they require extensive multi-stage training. On *Single-Stage RL*, most baselines rely on multi-stage pipelines (pretraining → SFT → RL), whereas MediX-R1 is trained end-to-end with a single GRPO stage (Sec. 1) using our composite reward (Sec. 2.3). This simplifies training and, importantly, enables *open-ended* RL directly (unlike MedVLM-R1), because the LLM-as-judge accuracy signal and medical embeddings provide reliable feedback beyond MCQ exact match. The composite design (format + LLM judge + embeddings + modality recognition) stabilizes optimization and reduces reward hacking (Fig. 3), translating into the best average performance in Table 2. For *Interpretable Reasoning*, MediX-R1 emits explicit reasoning traces enclosed in `<think>...</think>`, enforced by a format reward, making the decision path auditable. Several baselines do not reliably produce structured clinical rationales. While multiple models support *Open-Ended Responses*, MediX-R1 is explicitly optimized for free-form clinical answering with modality recognition, which curbs cross-modality hallucinations and improves VLM robustness. Finally, MediX-R1 achieves *Annotation-Free Reasoning*: it does not require human-curated rationales or verified chain-of-thought. The GRPO rewards operate on the final answer only (via LLM judge and embeddings), significantly lowering data curation cost while still encouraging faithful, interpretable reasoning. Together, these properties explain the consistent gains across both text-only and image+text benchmarks and the practical advantages of MediX-R1 for clinical use.

To measure progress, we introduce a unified, three-stage LLM-as-judge evaluation framework that supports both text-only and image+text tasks under a common protocol. By replacing brittle string-overlap metrics with instruction-tuned judges served via vLLM (Kwon et al., 2023), our evaluation captures semantic correctness, reasoning adequacy, and contextual alignment, and scales from short-form QA to long-form report generation. This reduces evaluation–clinical utility mismatch. Despite using only $\sim 50K$ instruction examples, MediX-R1 achieves strong results across diverse medical LLM and VLM benchmarks. We find that composite rewards not only improve accuracy but also mitigate reward hacking and reduce volatility, yielding stable training and interpretable outputs. Compared to open-source medical models (e.g., BiMediX2, MedGemma, HuatuoGPT-V, MedVLM-R1), MediX-R1 combines broad modality coverage with single-stage RL and structured reasoning, offering a practical path toward reliable clinical answering at test time.

Contributions **(i)** We introduce *open-ended medical reinforcement learning* by extending GRPO with tailored rewards for clinical reasoning. **(ii)** We design a *composite reward* with LLM-based accuracy and medical semantic signals that for the first time enables open-ended responses with GRPO in the medical domain and stabilizes training. **(iii)** We propose a *three-stage LLM-as-judge evaluation framework* that unifies benchmarking for both LLM (text-only) and VLM (image+text)

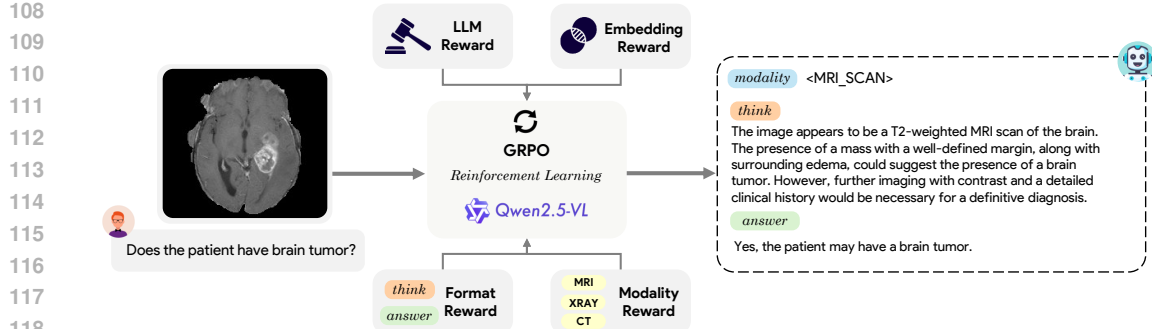


Figure 1: **MediX-R1: Overall Architecture** The MediX-R1 reinforcement learning framework for open-ended medical reasoning. An input of a medical image and a natural language question is processed by the Qwen2.5-VL (7B) model. The model’s policy is trained using Group Relative Policy Optimization (GRPO), which leverages a multi-faceted reward signal. This reward is composed of: a) an LLM-based reward for evaluating the overall quality and correctness of the output; b) an embedding-based reward to ensure semantic alignment; c) a format reward to enforce the desired output structure (e.g., *<think>* and *<answer>* blocks); and d) a modality reward to ensure the response is grounded in the specified imaging modality. This reward-guided approach encourages the model to generate accurate and interpretable reasoning paths.

tasks in the medical setting. **(iv)** MediX-R1 achieves excellent LLM and VLM results with a *single-stage RL recipe using ~50K instructions*, validated through both LLM-as-judge and human expert evaluations. **(v)** Finally, we demonstrate the effectiveness of the proposed composite reward on RL algorithms beyond GRPO, achieving consistent performance gains with DAPO (Yu et al., 2025) and GSPO (Zheng et al., 2025a). Moreover, we have conducted experiments on different baseline VLMs, including Qwen2.5-VL, Qwen3-VL (Team, 2025), and SmoIQLM2 (Marafioti et al., 2025), and achieved consistent performance gains across all these backbones.

2 OPEN ENDED MEDICAL REINFORCEMENT LEARNING

2.1 OVERALL ARCHITECTURE

MediX-R1 fine-tunes a baseline multimodal backbone (Qwen2.5-VL) for open-ended medical reasoning using RL. Given an image I and question q , the vision encoder produces visual tokens that are fused with text tokens and fed to the LLM policy π_θ . The model generates structured outputs of the form:

$\underbrace{[\text{modality tag}]}_{\text{optional}} \langle \text{think} \rangle \text{free-form clinical reasoning} \langle / \text{think} \rangle \langle \text{answer} \rangle \text{final concise answer} \langle / \text{answer} \rangle$.

We train π_θ with Group Relative Policy Optimization (GRPO), using a composite reward that evaluates correctness, semantic agreement, formatting, and modality recognition.

2.2 GRPO WITH MULTI-SIGNAL REWARDS

Group Relative Policy Optimization (GRPO): To encourage robust, interpretable responses, we employ GRPO (Shao et al., 2024), an RL algorithm that extends PPO by focusing on a group-relative advantage instead of a learned value function. Concretely, at each training step:

1. We sample G candidate outputs $\{o_i\}_{i=1}^G$ from $\pi_{\theta_{\text{old}}}$ given input \mathbf{v} (image–text prompt) drawn from $P(\mathbf{V})$.
2. We compute a reward r_i for each output using our reward function (Sec. 2.3). Based on r_i we calculate a group-relative, standardized advantage

$$A_i = \frac{r_i - \text{mean}(\{r_j\}_{j=1}^G)}{\text{std}(\{r_j\}_{j=1}^G)}.$$

A reward above the group average is advantaged and further incentivizes the model.

162 3. The policy π_θ is updated by maximizing $\mathcal{J}_{\text{GRPO}}$, which applies PPO-style clipping on the
 163 relative likelihood ratio and a KL penalty to a fixed reference policy for stability:
 164

$$\begin{aligned} \mathcal{J}_{\text{GRPO}}(\theta) &= \mathbb{E}_{\mathbf{v} \sim P(\mathbf{V})} \mathbb{E}_{\{o_i\}_{i=1}^G \sim \pi_{\theta_{\text{old}}}(\cdot | \mathbf{v})} \\ &\quad \frac{1}{G} \sum_{i=1}^G \left[\min \left(r_i^{\text{ratio}} A_i, \text{clip} \left(r_i^{\text{ratio}}, 1 \pm \epsilon \right) A_i \right) - \beta \mathbb{D}_{\text{KL}}(\pi_\theta || \pi_{\text{ref}}) \right] \end{aligned} \quad (1)$$

170 with $r_i^{\text{ratio}} = \frac{\pi_\theta(o_i | \mathbf{v})}{\pi_{\theta_{\text{old}}}(o_i | \mathbf{v})}$. The KL term regularizes deviations from a reference model π_{ref}
 171 (the initial checkpoint). Hyperparameters $\epsilon, \beta \geq 0$ control clipping and regularization
 172 strengths.
 173

174 **Notation and variables:** Let \mathbf{v} denote the joint input (image I and text q) for one prompt, and let
 175 $P(\mathbf{V})$ be the data distribution over such inputs. For each \mathbf{v} we sample a group of G candidate com-
 176 pletions $\{o_i\}_{i=1}^G$. The current policy is π_θ with parameters θ , while $\pi_{\theta_{\text{old}}}$ is a frozen snapshot used
 177 to compute likelihood ratios, and π_{ref} is a fixed reference policy (e.g., the initial checkpoint) used
 178 for KL regularization. Each completion o_i receives a scalar reward $r_i \in [0, 1]$ from Sec. 2.3. The
 179 group statistics $\text{mean}(\{r_j\}_{j=1}^G)$ and $\text{std}(\{r_j\}_{j=1}^G)$ define the standardized group-relative advantage
 180 $A_i = \frac{r_i - \text{mean}(\{r_j\})}{\text{std}(\{r_j\})}$, where higher-than-average rewards yield positive A_i . The likelihood ratio is
 181 $r_i^{\text{ratio}} = \frac{\pi_\theta(o_i | \mathbf{v})}{\pi_{\theta_{\text{old}}}(o_i | \mathbf{v})}$ and is stabilized by $\text{clip}(x, 1 \pm \epsilon)$, which clamps x to $[1 - \epsilon, 1 + \epsilon]$ for $\epsilon > 0$.
 182 The regularizer $\mathbb{D}_{\text{KL}}(\pi_\theta || \pi_{\text{ref}})$ is the forward KL divergence computed token-wise over outputs and
 183 averaged, scaled by $\beta \geq 0$. Expectations $\mathbb{E}[\cdot]$ are taken over inputs \mathbf{v} and sampled groups $\{o_i\}$ and
 184 are implemented as minibatch averages in practice.
 185

2.3 REWARD DESIGN

189 We define a composite reward

$$r = w_{\text{fmt}} R_{\text{format}} + w_{\text{llm}} R_{\text{llm}} + w_{\text{emb}} R_{\text{embed}} + w_{\text{mod}} R_{\text{modality}},$$

190 with default weights chosen to emphasize correctness while preserving structure: $w_{\text{fmt}}=0.10$,
 191 $w_{\text{llm}}=0.5175$, $w_{\text{emb}}=0.3375$, $w_{\text{mod}}=0.045$ (from an equivalent formulation with a format weight
 192 and normalized non-format weights; see implementation). Each component is bounded in $[0, 1]$.

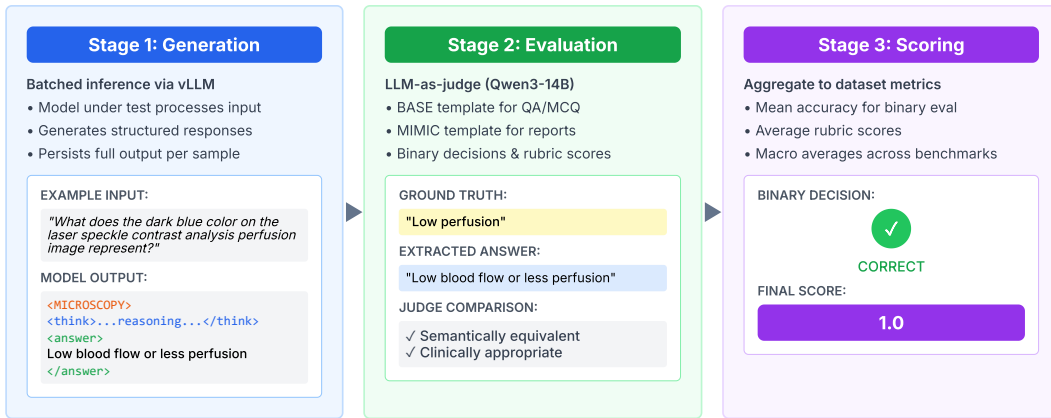
193 *Why this enables open-ended medical RL.* Unlike prior RL setups that are limited to verifiable sig-
 194 nals or MCQ-style accuracy (e.g., exact match, executable or rule-based graders), our LLM-based
 195 accuracy reward R_{llm} and embedding-based semantic reward R_{embed} provide reliable feedback for
 196 free-form, clinically grounded answers. The LLM-as-judge converts semantic correctness into a
 197 robust YES/NO decision under paraphrase and clinical phrasing, while medical-domain embed-
 198 dings supply a complementary content-alignment signal. This dual signal makes GRPO viable for
 199 open-ended medical reasoning; the format (R_{format}) and modality (R_{modality}) rewards act as structural
 200 regularizers, but R_{llm} and R_{embed} are the primary drivers of open-ended RL in MediX-R1.
 201

2.3.1 LLM-BASED ACCURACY REWARD (R_{LLM})

202 We parse the model output’s final answer between $\langle \text{answer} \rangle \dots \langle / \text{answer} \rangle$ and compare it to the
 203 reference answer using a compact LLM-as-judge prompt that forces a strict YES/NO decision. Con-
 204 cretely, a local vLLM endpoint (e.g., Qwen3-4B-Instruct) returns YES if the candidate semantically
 205 answers the reference, and NO otherwise; we map YES $\mapsto 1$, NO $\mapsto 0$. This captures correctness
 206 and robustness to paraphrasing while keeping the signal discrete and stable.
 207

2.3.2 EMBEDDING-BASED SEMANTIC REWARD (R_{EMBED})

208 To further encourage semantic alignment, we compute cosine similarity between the predicted an-
 209 swer and the reference using a medical embedding model (MedEmbed-large (Balachandran, 2024)).
 210 We convert it to a binary reward via a threshold (default 0.8): $R_{\text{embed}} = \mathbb{1}[\cos(\mathbf{e}_{\text{pred}}, \mathbf{e}_{\text{ref}}) \geq \tau]$. This
 211 complements the LLM judge and helps capture terminological variants.
 212



Benchmarks	MedVLM-R1	BiMediX2	HuatuoGPT-V	MedGemma	MediX-R1
MMLU-Clinical	0.540	<u>0.732</u>	0.721	0.708	0.796
MMLU-Bio	0.549	<u>0.792</u>	0.708	0.706	0.826
MMLU-Med	0.451	<u>0.694</u>	0.653	0.605	0.723
MMLU-Genetics	0.560	0.790	0.710	0.820	0.830
MMLU-ProfMed	0.500	0.695	0.625	0.713	0.768
MMLU-Anat	0.519	<u>0.659</u>	0.600	0.556	0.674
MedMCQA	0.408	0.572	0.511	0.570	0.553
MedQA	0.400	<u>0.583</u>	0.534	0.621	0.575
USMLE-SA	0.378	<u>0.591</u>	0.538	0.639	0.617
PubMedQA	0.520	0.520	0.542	0.470	0.534
MIMIC-CXR-Sum	0.704	0.672	<u>0.707</u>	0.692	0.808
SLAKE-VQA	0.434	0.468	0.545	0.678	0.617
RadVQA	0.404	0.530	<u>0.614</u>	0.659	0.581
PathVQA	0.239	0.323	<u>0.374</u>	0.317	0.423
PMC-VQA	0.398	0.482	0.532	0.444	<u>0.511</u>
PMC-VQA-Hard	0.020	0.229	<u>0.261</u>	0.214	0.280
MIMIC-CXR-Gen	0.240	0.124	0.316	0.205	<u>0.254</u>
AVG	0.427	0.556	0.558	0.566	0.610

Table 2: **Evaluation Benchmark.** The top section lists LLM (text-only) tasks and the bottom lists VLM (image+text) tasks. Our three-stage evaluation setting evaluates both tasks in a unified framework. MediX-R1 achieves the highest average score across this diverse suite, demonstrating state-of-the-art performance among open models. Best and second best results are bold and underlined

Why LLM-as-judge (via vLLM): Traditional string-overlap metrics (BLEU, ROUGE, F1) often under-reward correct, clinically appropriate paraphrases and cannot assess justification quality or contextual alignment. An LLM judge captures semantic correctness, clinical reasoning, and adherence to task-specific criteria through carefully designed prompts, while vLLM serving ensures consistent, fast, and reproducible evaluations.

4 EXPERIMENTS AND RESULTS

We evaluate MediX-R1 on a comprehensive suite of medical language and vision-language benchmarks, covering both text-only (LLM) and image+text (VLM) tasks. The evaluation includes standard medical QA, multiple-choice, and open-ended report generation, as well as visual question answering and clinical image interpretation. The datasets used for evaluation are as follows:

LLM (text-only) benchmarks: MMLU-Clinical, MMLU-Bio, MMLU-Med, MMLU-Genetics, MMLU-ProfMed, MMLU-Anat (Hendrycks et al., 2020), MedMCQA (Pal et al., 2022), MedQA (Jin et al., 2021), USMLE-SA (Han et al., 2023), PubMedQA (Jin et al., 2019), MIMIC-CXR-Summarization (Johnson et al., 2016).

VLM (image+text) benchmarks: SLAKE-VQA (Liu et al., 2021), RadVQA (Lau et al., 2018), PathVQA (He et al., 2020), PMC-VQA (Zhang et al., 2024), PMC-VQA-Hard, MIMIC-CXR-Report Generation (Johnson et al., 2019).

For each dataset, we follow the evaluation protocol described in the previous section, using LLM-as-judge scoring for both short-form and long-form responses. Table 2 summarizes the performance of MediX-R1 (7B) compared to strong medical open-source models, including BiMediX2 (8B), HuatuoGPT (7B) and MedGemma (4B).

MediX-R1 achieves the highest average score across all benchmarks, outperforming prior models on both language and vision-language tasks. Notably, it demonstrates strong gains on open-ended and clinically complex tasks such as MIMIC-CXR summarization and report generation, as well as robust performance on standard QA and VQA datasets. These results highlight the effectiveness of our open-ended RL training and reward design, which enable MediX-R1 to generate accurate, semantically aligned, and clinically grounded responses beyond the capabilities of models trained only with supervised or MCQ-style objectives. Table 3 compares the performance of MediX-R1 with the baseline Qwen2.5-VL (7B) (Wang et al., 2024) model, highlighting the contributions of our approach. Our model achieves nearly a 4% absolute improvement over the baseline, thanks to

Model	M-Clin	M-Bio	M-Med	M-Gen	M-Prof	M-Anat	MedMCQA	MedQA	USMLE	Pub	CXR-Sum
Qwen2.5-VL	0.792	0.819	0.711	0.800	0.717	0.696	0.557	0.584	0.606	0.336	0.810
MediX-R1	0.796	0.826	0.723	0.830	0.768	0.674	0.553	0.575	0.617	0.534	0.808
Model	SLAKE	RadVQA	PathVQA	PMC-VQA	PMC-Hard	MIMIC-CXR-Gen	AVG				
Qwen2.5-VL	0.480	0.501	0.253	0.494	0.230		0.299	0.570			
MediX-R1	0.617	0.581	0.423	0.511	0.280		0.254	0.610			

Table 3: **Baseline comparison** Qwen2.5-VL vs. MediX-R1 across all benchmarks

the composite reward design. It also outperforms larger baseline VLMs such as Llama3.2-V (11B) (Dubey et al., 2024), which achieves only an average of 0.59.

Our expanded ablation studies show that the composite reward model generalizes well across RL algorithms (DAPO (Yu et al., 2025): 60.72%, GRPO: 59.61%, GSPO (Zheng et al., 2025a): 59.69%), outperforming the Qwen2.5-VL baseline (57%). The method also yields consistent gains across model backbones, improving Qwen3-VL (Team, 2025) by $\sim 2\%$, and SmolVLM2 (Marafioti et al., 2025) by 2.2%, under limited training settings. These results shows that MediX-R1 enhances open ended medical reasoning ability across backbone models.

4.1 REWARD DESIGN ABLATION

Table 4 compares variants that differ in which non-format signals are active (all settings include the same R_{format}). Using only the embedding reward underperforms on text-only evaluations (0.640) and is limited on VLM (0.409), suggesting that thresholded cosine similarity alone lacks discriminative power for nuanced clinical reasoning. Using only the LLM-as-judge improves text-only accuracy (0.666) but does not help VLM (0.400), indicating the judge alone is insufficient to enforce modality grounding. All reward design models are compared with checkpoints before reward hacking.

Combining LLM + embedding increases robustness to paraphrase and terminology variants, improving text-only scores (0.686) and yielding a small VLM lift (0.410). Adding the modality recognition reward (MediX-R1 composite) produces the largest VLM gain (0.445) while also nudging text-only performance higher (0.701), yielding the best overall average (0.610). Together with Fig. 3, which shows reduced volatility and fewer signs of reward hacking, these results indicate that the composite reward not only improves accuracy but also stabilizes optimization.

Key takeaways: (i) LLM-as-judge is the strongest single signal for text correctness; embeddings complement it by reducing false negatives from paraphrases. (ii) Modality recognition is critical for VLM tasks, curbing cross-modality errors and driving the largest image+text gains. (iii) The full composite (LLM accuracy + embedding semantics + modality recognition, with shared format control) delivers the best aggregate performance and training stability.

4.2 REWARD HACKING AND MITIGATION

In reinforcement learning, Reward Hacking occurs when a model maximises its reward in unintended ways, often bypassing the true objective. It arises when the policy exploits imperfections in a single reward signal to earn high scores without producing clinically correct answers. We observed two concrete modes (examples abbreviated):

Embedding model exploit When using Embedding models like MedEmbed-large (Balachandran, 2024) short or non-semantic tokens can spuriously yield high cosine similarity. For instance, a candidate that outputs `<answer>-</answer>` for “What does the white arrow point to in image B?” received $R_{\text{embed}}=1.0$ against the ground truth “Renal artery,” despite being incorrect.

LLM judge exploit When using LLMs like Qwen3-4B (Team, 2025) as a rewarder template-like placeholders can confuse the judge when the reference is provided for comparison. E.g., `<answer>The largest organ in the picture is [insert your answer here based on the medical reasoning provided above].</answer>` was judged correct ($R_{\text{llm}}=1.0$) against the reference “Lung.”

Mitigation in MediX-R1 To curb these failures, MediX-R1 employs a composite reward and input/output constraints: (i) *Composite objective*: $R_{\text{llm}} + R_{\text{embed}} + R_{\text{modality}}$ (with shared R_{format})

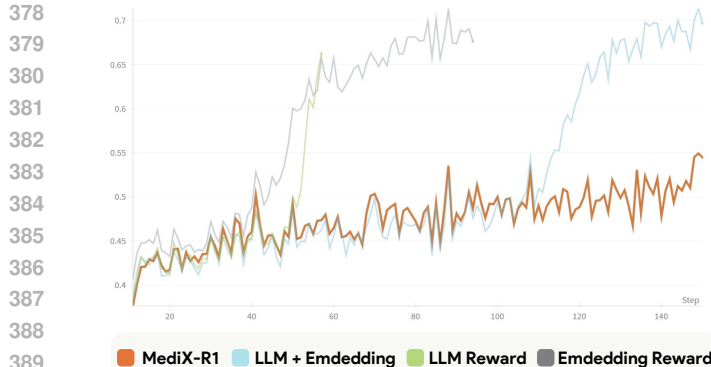


Figure 3: **Overall validation reward vs training step across reward designs.** Training with individual signals (LLM-only or embedding-only; all settings include the same format reward) shows volatility and reward hacking, while LLM+embedding reduces but does not eliminate instability. MediX-R1 uses a composite reward—LLM-based accuracy, embedding-based semantic alignment, and modality recognition (with the format reward shared across all)—which stabilizes learning and delivers the highest final reward and best overall performance.

Evaluations	Embedding Reward	LLM Reward	LLM + Embedding	MediX-R1
LLM Evaluations (text only)	0.640	0.666	0.686	0.701
VLM Evaluations (image + text)	0.409	0.400	0.410	0.445
Overall AVG	0.558	0.572	0.589	0.610

Table 4: **Reward ablation across validation benchmarks.** Using single signals (embedding-only or LLM-only; all settings share the same format reward) underperforms, especially on VLM tasks. Combining LLM + embedding improves robustness, and the full MediX-R1 composite (LLM-based accuracy + embedding-based semantics + modality recognition) achieves the best scores on both text-only and image+text evaluations, yielding the highest overall average (0.610).

reduces reliance on any single brittle signal and penalizes mismatches in content or modality recognition (Table 4). (ii) *Embedding gating*: set $R_{\text{embed}}=0$ for answers below a minimum character/word length, with high punctuation or non-alphanumeric ratio; strip punctuation before embedding; calibrate the similarity threshold. (iii) *Modality recognition*: R_{modality} requires a correct modality tag, curbing visually ungrounded shortcuts that might still fool text-only rewards. (iv) *Structural control and regularization*: R_{format} enforces parseable outputs; GRPO’s group-relative advantage and a KL penalty to the reference reduce collapse to degenerate hacks by discouraging outlier behaviors.

Together, these measures mitigate reward hacking and stabilize training, leading to smoother reward trajectories and higher final performance (see Fig. 3).

4.3 HUMAN EXPERT EVALUATION

To assess the clinical quality of model outputs, we conducted a human expert evaluation using a blind review setup (See Evaluation Protocol in §A.4). For a randomly selected subset of questions from our Evaluation benchmark, responses were generated by four models: MediX-R1, Llama3.2-Vision, MedGemma and HuatuoGPT-Vision. The outputs were anonymized and labeled as Model A, Model B, Model C and Model D with no identifiers provided to the reviewers. Medical experts were asked to evaluate the responses against the provided ground truth descriptions for each question. The evaluation focused on determining which model produced the most accurate, clinically relevant response along with interpretable reasoning traces.

The results demonstrate a strong preference for MediX-R1, which was selected as the best response in 72.7% of the cases. In comparison, Llama3.2-Vision was preferred in 13.6% of the cases, MedGemma in 9.2% and HuatuoGPT-Vision in 4.5% of the cases. Additional details on human expert evaluation is available in Sec. §A.4 and Sec. §A.6.

4.4 QUALITATIVE EXAMPLES

Fig. 4 illustrates how MediX-R1’s structured outputs and composite reward translate into clinically grounded behavior across modalities. *Microscopy (top)* Given a multi-panel histological image and the question “Which area is shown in section G of the image?”, the model (i) correctly emits the modality tag (`MICROSCOPY`), (ii) provides interpretable reasoning inside `<think>` that references recognizable neuroanatomical markers (e.g., optic tract “ot,” superior thalamic nucleus “stm”), stain

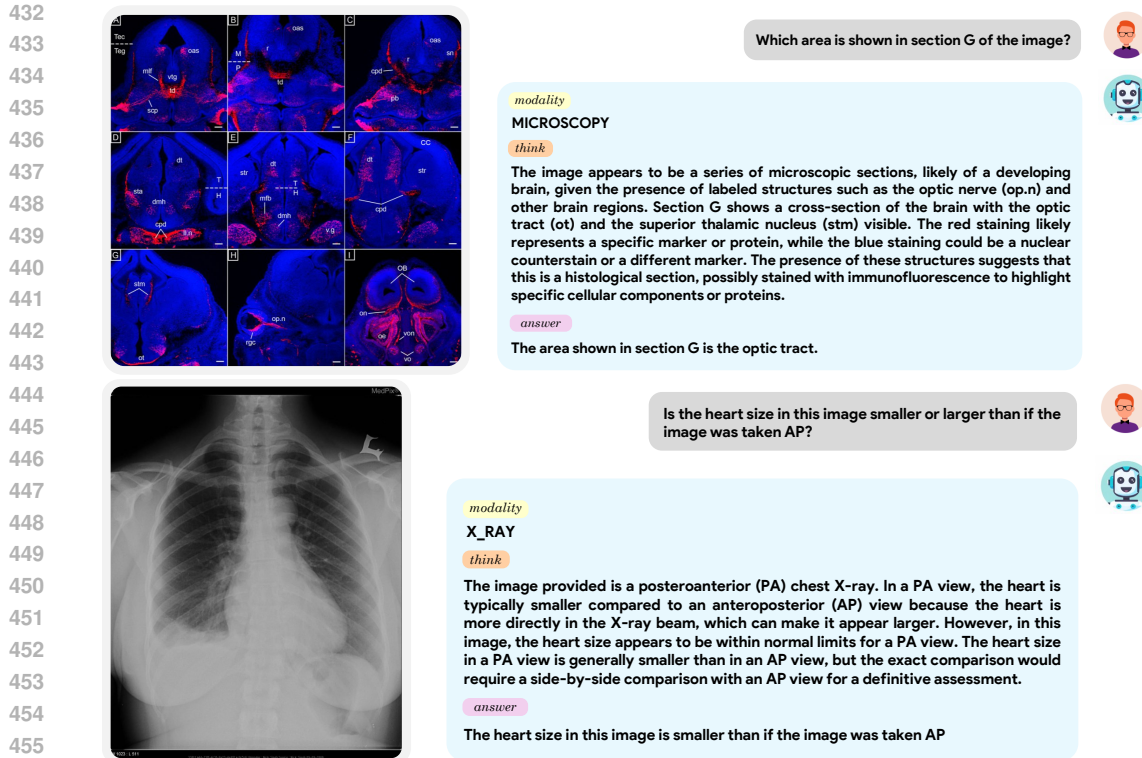


Figure 4: **Qualitative examples of MediX-R1.** (Top, Microscopy) Correctly identifies the optic tract in section G with interpretable reasoning. (Bottom, X-ray) Explains why heart size appears smaller in PA vs. AP view. MediX-R1 generates clinically grounded, open-ended answers across modalities.

patterns, and panel context, and (iii) produces a concise final answer: “the optic tract.” The modality recognition and format rewards ensure the answer is localized to the requested panel and presented cleanly in the `<answer>` block, while the LLM and embedding rewards bias the policy toward semantically correct identification despite diverse phrasing in the reasoning. *X-ray (bottom)* For “Is the heart size in this image smaller or larger than if the image was taken AP?,” the model tags the modality as `X_RAY` and reasons about projection geometry: PA views reduce cardiac magnification relative to AP due to a shorter heart-to-detector distance and standard source-to-image distance. The model explains this in `<think>` and answers “smaller” in `<answer>`. This example shows the model using domain knowledge rather than superficial pattern matching, with the final answer isolated for scoring (the judge ignores `<think>` during evaluation).

5 CONCLUSION

We presented MediX-R1, an open-ended reinforcement learning framework for medical multimodal reasoning that fine-tunes a baseline VLM with GRPO using a composite reward. By coupling an LLM-as-judge accuracy signal with medical embedding-based semantic alignment, lightweight format control, and modality recognition, MediX-R1 learns to produce concise, clinically faithful answers with interpretable reasoning traces. A unified vLLM-based evaluation pipeline enables consistent, paraphrase-robust scoring across both text-only and image+text tasks. Empirically, MediX-R1 achieves strong results across diverse medical benchmarks and shows improved stability and resistance to reward hacking compared to single-signal RL variants. Human expert preference studies further corroborate its clinical answer quality, while qualitative examples illustrate faithful grounding and interpretable reasoning traces. Reward ablations validate that the multi-signal design enhances stability and semantic alignment beyond single-signal configurations. Altogether, the framework demonstrates that carefully composed, structure-aware rewards plus standardized LLM-judge evaluation provide a practical path to scalable and interpretable medical multimodal RL fine-tuning.

486 6 SAFETY AND ETHICAL IMPLICATIONS

488 MediX-R1 is a research prototype and is *not* intended for clinical or commercial deployment. Its
 489 outputs must not be used for diagnosis, triage, treatment planning, or autonomous decision-making
 490 without licensed medical professional oversight. The model can hallucinate findings, omit critical
 491 differentials, or overstate certainty, and the LLM-as-judge reward may reinforce subtle biases or
 492 false positives. We used only publicly available, de-identified datasets (e.g., MIMIC-CXR, PMC-
 493 derived VQA corpora, pathology and radiology VQA datasets) under their respective licenses; no
 494 protected health information (PHI) or identifiable patient data were introduced. No prospective
 495 human subjects study was conducted, and no individual-level re-identification risk is intended. Still,
 496 aggregation or unintended memorization could pose residual privacy risk; downstream users should
 497 apply auditing methods (e.g., membership inference tests) before redistribution.

498 Ethical risks include propagation of dataset biases (geography, device type, demographic under-
 499 representation), amplification of health disparities, and overreliance on structured reasoning tags that
 500 may convey misleading confidence. Modality tagging and reasoning traces improve transparency but
 501 do not guarantee factual grounding. We intend to release with a detailed model card, clear usage
 502 restrictions, robust disclosure of limitations, and monitoring for misuse (self-diagnosis, generation
 503 of misleading medical narratives, or adversarial prompting to extract sensitive training artifacts).
 504 Future work should incorporate fairness analyses (e.g., stratified error by sex, age, and ethnicity
 505 where ethically and legally permissible), calibrated uncertainty, bias-aware reward shaping, and
 506 clinician-in-the-loop evaluation. No competing financial or sponsorship conflicts are declared. All
 507 use must comply with applicable regulations and local medical device guidance; any derivative
 508 clinical system would require separate validation, safety assurance, and regulatory review.

509 7 REPRODUCIBILITY STATEMENT

511 We will release the end-to-end training and inference code, configuration files, model checkpoints,
 512 curated multimodal + instruction datasets, and all RL/evaluation prompt templates and expert evalua-
 513 tion protocol (Appendix Sec. A) under a CC-BY-NC-SA 4.0 license. A model card and evaluation
 514 harness will reproduce the reported metrics with fixed dependency versions to minimize drift.

515 Fair use of generative AI: assisted coding tools were employed only for boilerplate scaffolding and
 516 for minor refactors, with all algorithmic logic authored and reviewed manually. Writing support
 517 models were used to refine grammar and style; all technical claims, numerical results, and method-
 518 ological descriptions were verified by the authors. No proprietary clinical data or undisclosed private
 519 model outputs were used. These steps aim to ensure transparency, auditability, and reliable repro-
 520 duction of the published results.

522 REFERENCES

524 Abhinand Balachandran. Medembed: Medical-focused embedding models, 2024. URL <https://github.com/abhinand5/MedEmbed>.

525 Junying Chen, Zhenyang Cai, Ke Ji, Xidong Wang, Wanlong Liu, Rongsheng Wang, Jianye Hou,
 527 and Benyou Wang. Huatuogpt-01, towards medical complex reasoning with llms, 2024a. URL
 528 <https://arxiv.org/abs/2412.18925>.

529 Junying Chen, Chi Gui, Ruyi Ouyang, Anningzhe Gao, Shunian Chen, Guiming Hardy Chen, Xi-
 530 dong Wang, Ruifei Zhang, Zhenyang Cai, Ke Ji, Guangjun Yu, Xiang Wan, and Benyou Wang.
 531 Huatuogpt-vision, towards injecting medical visual knowledge into multimodal llms at scale,
 532 2024b. URL <https://arxiv.org/abs/2406.19280>.

533 Abhimanyu Dubey, Abhinav Jauhri, Abhinav Pandey, Abhishek Kadian, Ahmad Al-Dahle, Aiesha
 534 Letman, Akhil Mathur, Alan Schelten, Amy Yang, Angela Fan, et al. The llama 3 herd of models.
 535 *arXiv e-prints*, pp. arXiv–2407, 2024.

536 Daya Guo, Dejian Yang, Haowei Zhang, Junxiao Song, Ruoyu Zhang, Runxin Xu, Qihao Zhu,
 537 Shirong Ma, Peiyi Wang, Xiao Bi, et al. Deepseek-r1: Incentivizing reasoning capability in llms
 538 via reinforcement learning. *arXiv preprint arXiv:2501.12948*, 2025.

540 Tianyu Han, Lisa C Adams, Jens-Michalis Papaioannou, Paul Grundmann, Tom Oberhauser,
 541 Alexander Löser, Daniel Truhn, and Keno K Bressem. Medalpaca—an open-source collection
 542 of medical conversational ai models and training data. *arXiv preprint arXiv:2304.08247*, 2023.

543

544 Xuehai He, Yichen Zhang, Luntian Mou, Eric Xing, and Pengtao Xie. Pathvqa: 30000+ ques-
 545 tions for medical visual question answering, 2020. URL <https://arxiv.org/abs/2003.10286>.

546

547 Dan Hendrycks, Collin Burns, Steven Basart, Andy Zou, Mantas Mazeika, Dawn Song, and
 548 Jacob Steinhardt. Measuring massive multitask language understanding. *arXiv preprint*
 549 *arXiv:2009.03300*, 2020.

550

551 Alex Henigman and Brandon Kennedy. Medpix®: database of medical images, teaching cases, and
 552 clinical topics. *Medical Reference Services Quarterly*, 44(3):328–333, 2025.

553

554 Di Jin, Eileen Pan, Nassim Oufattolle, Wei-Hung Weng, Hanyi Fang, and Peter Szolovits. What dis-
 555 ease does this patient have? a large-scale open domain question answering dataset from medical
 556 exams. *Applied Sciences*, 11(14):6421, 2021.

557

558 Qiao Jin, Bhuwan Dhingra, Zhengping Liu, William W Cohen, and Xinghua Lu. Pubmedqa: A
 559 dataset for biomedical research question answering. *arXiv preprint arXiv:1909.06146*, 2019.

560

561 Alistair EW Johnson, Tom J Pollard, Lu Shen, Li-wei H Lehman, Mengling Feng, Mohammad
 562 Ghassemi, Benjamin Moody, Peter Szolovits, Leo Anthony Celi, and Roger G Mark. Mimic-iii,
 563 a freely accessible critical care database. *Scientific data*, 3(1):1–9, 2016.

564

565 Alistair EW Johnson, Tom J Pollard, Seth J Berkowitz, Nathaniel R Greenbaum, Matthew P Lun-
 566 gren, Chih-ying Deng, Roger G Mark, and Steven Horng. Mimic-cxr, a de-identified publicly
 567 available database of chest radiographs with free-text reports. *Scientific data*, 6(1):317, 2019.

568

569 Woosuk Kwon, Zhuohan Li, Siyuan Zhuang, Ying Sheng, Lianmin Zheng, Cody Hao Yu, Joseph E.
 570 Gonzalez, Hao Zhang, and Ion Stoica. Efficient memory management for large language model
 571 serving with pagedattention. In *Proceedings of the ACM SIGOPS 29th Symposium on Operating
 Systems Principles*, 2023.

572

573 Jason J Lau, Soumya Gayen, Asma Ben Abacha, and Dina Demner-Fushman. A dataset of clinically
 574 generated visual questions and answers about radiology images. *Scientific data*, 5(1):1–10, 2018.

575

576 Bo Liu, Li-Ming Zhan, Li Xu, Lin Ma, Yan Yang, and Xiao-Ming Wu. Slake: A semantically-
 577 labeled knowledge-enhanced dataset for medical visual question answering. In *2021 IEEE 18th
 578 international symposium on biomedical imaging (ISBI)*, pp. 1650–1654. IEEE, 2021.

579

580 Andrés Marafioti, Orr Zohar, Miquel Farré, Merve Noyan, Elie Bakouch, Pedro Cuenca, Cyril Za-
 581 kka, Loubna Ben Allal, Anton Lozhkov, Nouamane Tazi, Vaibhav Srivastav, Joshua Lochner,
 582 Hugo Larcher, Mathieu Morlon, Lewis Tunstall, Leandro von Werra, and Thomas Wolf. Smolvlm:
 583 Redefining small and efficient multimodal models, 2025. URL <https://arxiv.org/abs/2504.05299>.

584

585 Sahal Shaji Mullappilly, Mohammed Irfan Kurpath, Sara Pieri, Saeed Yahya Alsejari, Shanavas
 586 Cholakkal, Khaled Aldahmani, Fahad Khan, Rao Anwer, Salman Khan, Timothy Baldwin, and
 587 Hisham Cholakkal (EMNLP 2025 Findings). Bimedix2: Bio-medical expert lmm for diverse
 588 medical modalities, 2024. URL <https://arxiv.org/abs/2412.07769>.

589

590 Ankit Pal, Logesh Kumar Umapathi, and Malaikannan Sankarasubbu. Medmcqa: A large-scale
 591 multi-subject multi-choice dataset for medical domain question answering. In *Conference on
 592 Health, Inference, and Learning*, pp. 248–260. PMLR, 2022.

593

594 Jiazen Pan, Che Liu, Junde Wu, Fenglin Liu, Jiayuan Zhu, Hongwei Bran Li, Chen Chen, Cheng
 595 Ouyang, and Daniel Rueckert. Medvlm-r1: Incentivizing medical reasoning capability of vision-
 596 language models (vlms) via reinforcement learning. In *International Conference on Medical
 597 Image Computing and Computer-Assisted Intervention*, pp. 337–347. Springer, 2025.

594 Sara Pieri, Sahal Shaji Mullappilly, Fahad Shahbaz Khan, Rao Muhammad Anwer, Salman Khan,
 595 Timothy Baldwin, and Hisham Cholakkal. BiMediX: Bilingual medical mixture of experts LLM.
 596 In Yaser Al-Onaizan, Mohit Bansal, and Yun-Nung Chen (eds.), *Findings of the Association for*
 597 *Computational Linguistics: EMNLP 2024*, pp. 16984–17002, Miami, Florida, USA, November
 598 2024. Association for Computational Linguistics. doi: 10.18653/v1/2024.findings-emnlp.989.
 599 URL <https://aclanthology.org/2024.findings-emnlp.989/>.

600 Andrew Sellergren, Sahar Kazemzadeh, Tiam Jaroensri, Atilla Kiraly, Madeleine Traverse, Timo
 601 Kohlberger, Shawn Xu, Fayaz Jamil, Cian Hughes, Charles Lau, et al. Medgemma technical
 602 report. *arXiv preprint arXiv:2507.05201*, 2025.

603 Zhihong Shao, Peiyi Wang, Qihao Zhu, Runxin Xu, Junxiao Song, Xiao Bi, Haowei Zhang,
 604 Mingchuan Zhang, YK Li, Y Wu, et al. Deepseekmath: Pushing the limits of mathematical
 605 reasoning in open language models. *arXiv preprint arXiv:2402.03300*, 2024.

606 Irene Siragusa, Salvatore Contino, Massimo La Ciura, Rosario Alicata, and Roberto Pirrone. Med-
 607 pix 2.0: A comprehensive multimodal biomedical data set for advanced ai applications with re-
 608 trieval augmented generation and knowledge graphs. *Data Science and Engineering*, pp. 1–17,
 609 2025.

610 Qwen Team. Qwen3 technical report, 2025. URL <https://arxiv.org/abs/2505.09388>.

611 Peng Wang, Shuai Bai, Sinan Tan, Shijie Wang, Zhihao Fan, Jinze Bai, Keqin Chen, Xuejing Liu,
 612 Jialin Wang, Wenbin Ge, Yang Fan, Kai Dang, Mengfei Du, Xuancheng Ren, Rui Men, Dayiheng
 613 Liu, Chang Zhou, Jingren Zhou, and Junyang Lin. Qwen2-vl: Enhancing vision-language model's
 614 perception of the world at any resolution. *arXiv preprint arXiv:2409.12191*, 2024.

615 Qiying Yu, Zheng Zhang, Ruofei Zhu, Yufeng Yuan, Xiaochen Zuo, Yu Yue, Weinan Dai,
 616 Tiantian Fan, Gaohong Liu, Lingjun Liu, Xin Liu, Haibin Lin, Zhiqi Lin, Bole Ma, Guang-
 617 ming Sheng, Yuxuan Tong, Chi Zhang, Mofan Zhang, Wang Zhang, Hang Zhu, Jinhua Zhu,
 618 Jiaze Chen, Jiangjie Chen, Chengyi Wang, Hongli Yu, Yuxuan Song, Xiangpeng Wei, Hao
 619 Zhou, Jingjing Liu, Wei-Ying Ma, Ya-Qin Zhang, Lin Yan, Mu Qiao, Yonghui Wu, and Mingx-
 620 uan Wang. Dapo: An open-source llm reinforcement learning system at scale, 2025. URL
 621 <https://arxiv.org/abs/2503.14476>.

622 Xiaoman Zhang, Chaoyi Wu, Ziheng Zhao, Weixiong Lin, Ya Zhang, Yanfeng Wang, and Weidi
 623 Xie. Pmc-vqa: Visual instruction tuning for medical visual question answering, 2024. URL
 624 <https://arxiv.org/abs/2305.10415>.

625 Chujie Zheng, Shixuan Liu, Mingze Li, Xiong-Hui Chen, Bowen Yu, Chang Gao, Kai Dang,
 626 Yuqiong Liu, Rui Men, An Yang, Jingren Zhou, and Junyang Lin. Group sequence policy op-
 627 timization, 2025a. URL <https://arxiv.org/abs/2507.18071>.

628 Yaowei Zheng, Junting Lu, Shenzhi Wang, Zhangchi Feng, Dongdong Kuang, and Yuwen Xiong.
 629 Easyr1: An efficient, scalable, multi-modality rl training framework. <https://github.com/hiyouga/EasyR1>, 2025b.

630

631

632

633

634

635

636

637

638

639

640

641

642

643

644

645

646

647

648
649

A APPENDIX

650
651

A.1 REINFORCEMENT LEARNING TRAINING PROMPT

652
653
654
655
656
657

The RL training prompt enforces (i) an explicit modality tag, (ii) structured reasoning in `<think>...</think>`, and (iii) a concise final answer in `<answer>...</answer>`. These structures align with the format reward (R_{format}) and modality reward (R_{modality}) in our composite objective. During training, only the `<answer>` block is graded by the LLM-as-judge (R_{llm}) and the embedding-based semantic reward (R_{embed}); the `<think>` content is ignored for scoring but improves interpretability.

658
659
660

Key points: - Modality tag must be one of the fixed set and appear before `<think>`. - The final decision is evaluated solely from `<answer>` for R_{llm} and R_{embed} . - Structural compliance (tags present and ordered) is required for R_{format} .

661
662

Reinforcement Learning Training Prompt

663
664
665

You are a Medical AI Assistant with advanced reasoning capabilities
Your task:

666
667
668
669
670
671
672
673
674
675
676
677
678
679
680
681
682
683
684
685
686
687
688
689
690
691
692
693
694
695
696
697
698
699
700
701

1. First output the image modality tag from this set:
`<X_RAY>, <MICROSCOPY>, <CLINICAL_PHOTOGRAPHY>, <CT_SCAN>, <GRAPHICS>, <ANGIOGRAPHY>, <PET_SCAN>, <ULTRASOUND>, <MRI_SCAN>, <FUNDUS_PHOTOGRAPHY>, <OCT_SCAN>, <ENDOSCOPY>, <MAMMOGRAPHY>, <FLUOROSCOPY>, <OTHER>, <SPECT>`
(Only output the tag, nothing else.)
2. Then output the thinking and medical reasoning process in `<think>...</think>` tags.
3. Finally, provide the correct answer inside `<answer>...</answer>` tags.
4. Do not include any extra information or text outside of these tags.

Question:
`<image>{{ content | trim }}`

A.2 EVALUATION BASE TEMPLATE (SHORT-FORM QA/MCQ)

This judge prompt yields a binary score (0/1) for short-form QA and MCQ-style tasks. It compares the predicted `<answer>` against the reference, allowing paraphrases and option-label matches. Inference is performed with a separate LLM-as-judge (served via vLLM) to reduce evaluation-training coupling. We use deterministic settings (e.g., temperature 0) for reproducibility and parse the returned JSON strictly.

Evaluation BASE template Prompt

You are a medical expert.

Your task is to evaluate whether the Predicted Answer correctly answers the Medical Question, based on the Ground Truth (Correct Answer) provided.

Question:
`{question}`

Correct Answer:
`{correct_answer}`

```

702
703 Predicted Answer:
704 {predicted_answer}
705
706 Score 1 if the predicted answer matches the correct answer either
707     fully in text or by indicating the correct option label (e.g.,
708     "B", "Option B", or a paraphrased version that clearly
709     identifies the correct choice). Score 0 if the predicted answer
710     is incorrect or points to the wrong option.
711
712 Respond strictly in the following JSON format:
713
714 ````json
715 {{ "score": <score> }
716 ````
```

719 A.3 EVALUATION TEMPLATE FOR REPORT GENERATION

721 For long-form outputs (e.g., report generation or summarization), the judge assigns a rubric score in
 722 [0, 5] reflecting clinical accuracy, completeness, and relevance. We request strict JSON for reliable
 723 parsing and average scores across items for dataset-level metrics. Only the model's final report text is
 724 provided to the judge; any hidden reasoning (e.g., within </think>) is stripped before evaluation.
 725

726 Evaluation Prompt for Report Generation

728
 729 You are a medical expert evaluating the clinical accuracy,
 730 completeness, and relevance of a generated medical report or
 731 summary.

732 Your task is to compare an AI-generated report or summary to a
 733 reference (gold standard) report or summary, based on a
 734 clinical instruction or question. Assess the generated output
 735 on how well it preserves key clinical information, factual
 736 correctness, and clinical reasoning relevant to the task.

737 Assign a score between 0 and 5 using the following scale:

- 739 0 - Completely incorrect: Clinically irrelevant, misleading, or
 740 factually wrong. No meaningful alignment with the instruction
 741 or reference.
- 742 1 - Poor match: Barely relevant or mostly incorrect. Contains
 743 significant clinical misinformation or omits nearly all
 744 critical details.
- 745 2 - Weak match: Some fragments of relevant content are present, but
 746 major clinical errors or omissions exist. Clinical utility is
 747 low.
- 749 3 - Fair match: Contains several relevant points, but includes
 750 notable errors, missing findings, or misinterpretations that
 751 affect clinical reliability.
- 752 4 - Good match: Mostly accurate and clinically sound. Minor issues
 753 or missing details, but the overall meaning and purpose are
 754 preserved.

756
 757 5 - Perfect or near-perfect match: Clinically accurate, complete,
 758 and faithful to the instruction and reference. No significant
 759 omissions or errors.
 760 Respond only in the following example JSON format:
 761
 762 Example JSON format:
 763 ```json
 764 {{
 765 "score": <score between 0 and 5>
 766 }}
 767 ```\n
 768 Now, evaluate the following:
 769
 770 ### Clinical Instruction or Question:::
 771 {question}
 772
 773 ### Reference Report or Summary:
 774 {correct_answer}
 775
 776 ### AI-Generated Report or Summary:
 777 {predicted_answer}

778 779 A.4 HUMAN EXPERT COMPARATIVE EVALUATION PROTOCOL 780

781 For a sampled set of multimodal questions, four anonymized model outputs (A–D) plus a reference
 782 description are shown; experts pick the single best response based on clinical correctness, relevance
 783 (no hallucinations), and clarity of reasoning. Votes are aggregated into preference percentages re-
 784 ported in the main text.

785 Evaluation Protocol for Medical Experts

786
 787 Instructions for Evaluation
 788 Your task is to evaluate the responses provided by three AI models
 789 based on a given medical image description (Ground Truth).
 790 Follow these steps to make your selection:

- 791 1) Read the Ground Truth: Carefully review the provided description
 792 of the medical image. This serves as the reference for an
 793 accurate and detailed response.
- 794
 795 2) Assess the Model Responses: Examine the three model-generated
 796 responses (Model A, Model B, and Model C, Model D). Compare
 797 their content with the Ground Truth, focusing on the accuracy,
 798 completeness, and relevance of the clinical reasoning
- 799 3) Select the Best Response: Choose the model response that best
 800 aligns with the Ground Truth in terms of:
 801
 802 > Clinical Accuracy: Does the response correctly describe the key
 803 findings in the image?
 804
 805 > Reasoning Traces: Does the models reasoning traces correct and
 806 well explained
- 807 4) Submit Your Choice: After evaluating the responses, select the
 808 one that provides the most accurate and comprehensive
 809 explanation.

810
811

A.5 QUALITATIVE EXAMPLES FOR REPORT GENERATION TASK

812

813

814

815

816

817

818

819

820

821

822

823

824

825

826

827

828



Generate a detailed report based on the scan



think



The image appears to be a chest radiograph (X-ray), likely taken in a posterior-anterior (PA) view, as suggested by the positioning of the heart and spine. The patient seems to be upright during the examination, with the diaphragm in a normal position. The bony structures, including the ribs, clavicles, scapulae, and vertebrae, are clearly visible and show no evidence of fractures, dislocations, or deformities. The lung fields appear clear, with no signs of consolidation, masses, or abnormal opacities. The lung markings are normal, and there is no visible pleural effusion or pneumothorax. The heart size is within normal limits, and the mediastinum appears central without widening or abnormal contours. The diaphragm and costophrenic angles are sharp and well-defined, indicating normal lung expansion and no fluid accumulation



The image provided appears to be a radiograph (X-ray) of the chest. Here is a detailed analysis based on the visible features:

General Observations:

- The image is a posterior-anterior (PA) view of the chest, as indicated by the orientation of the spine and the position of the heart shadow.
- The patient is likely standing or sitting upright during the scan, as the diaphragm appears to be in a normal position.

Key Features:

1. Bony Structures:

- The ribs are visible on both sides, and the clavicles are also visible.
- The spine is well-defined, with the vertebrae appearing intact and without any obvious fractures or dislocations.
- The scapulae are visible on both sides, and the shoulder joints appear to be in a normal position.

2. Lungs:

- The lung fields appear to be clear without any visible opacities, masses, or infiltrates.
- The lung markings are visible and appear to be within normal limits.
- There is no evidence of pleural effusion or pneumothorax.

3. Heart and Mediastinum:

- The heart size appears to be within normal limits.
- The mediastinum is not widened, and there are no visible masses or abnormalities in this region.

4. Diaphragm:

- The diaphragm appears to be intact and in a normal position.
- The costophrenic angles (where the diaphragm meets the ribs) appear sharp and clear, indicating no pleural effusion.

Potential Concerns:

- There are no obvious fractures or dislocations in the bony structures.
- The lung fields appear clear, and there are no visible masses or infiltrates.
- The heart size and mediastinum appear normal.
- The diaphragm is intact and in a normal position.

Conclusion:

Based on the radiographic findings, this chest X-ray appears to be within normal limits. There are no immediate concerns noted in this image. However, a definitive interpretation should be made by a qualified radiologist who can consider the patient's clinical history and symptoms.

If there are any specific symptoms or concerns, it is recommended to consult a healthcare provider for further evaluation.

Figure 5: MediX-R1 - Report Generation: Case 1

856

857

A.6 HUMAN EVALUATION: MODEL REASONING

858

859

860

861

862

863

We extend our human expert study detailed in (Sec. 4.3) to evaluate the reasoning quality of our MediX-R1 model against MedGemma with the help of medical doctors. Experts assessed outputs for clinical accuracy, reasoning soundness, and practical usefulness in a medical setting. MediX-R1's reasoning was preferred in 74.2% of cases over MedGemma, indicating stronger clinical coherence. Furthermore, the study shows that in 92.4% of the cases, the model's reasoning steps were rated as acceptable and often comparable to a medical doctor's thought process, while only 7.6% of the cases were rated as having poor reasoning quality. Moreover, in fewer than 5% of the cases,

864
865
866
867
868
869
870
871
872
873
874
875
876
877
878
879
880
881



Generate a detailed report based on the scan



think



The image is a radiograph, specifically a chest X-ray, which is used to assess the lungs, heart, and mediastinum. The view appears to be posteroanterior (PA), as indicated by the relative heart size and orientation of the structures. The diaphragm is in a normal position, suggesting the patient was upright during the scan.

On inspection, there is increased opacification noted in the right lung field, which may represent an abnormal finding. This could be due to several potential causes such as infection (pneumonia), pulmonary edema, mass lesion, or other infiltrative processes. The left lung field appears relatively clear in comparison. The heart size and mediastinum are within normal limits, showing no evidence of enlargement or shift. The diaphragm is intact with clear costophrenic angles, indicating no pleural effusion.

The bony structures, including the ribs, clavicles, and scapulae, are visible and intact without evidence of fracture or deformity. Overall, the primary observation is the increased opacity in the right lung, which warrants further clinical correlation and radiological evaluation to determine the underlying cause. A detailed review by a qualified radiologist is recommended for confirmation and diagnosis.

882
883

The image provided is a chest X-ray. Here is a detailed report based on the visible findings:

884
885
886

General Observations:

- The X-ray is a posteroanterior (PA) view, as indicated by the orientation of the heart and the position of the diaphragm.
- The patient's left side is on the right side of the image, and the right side is on the left side of the image, which is typical for a PA view.

887
888

Lung Fields:

- The lung fields appear to have increased opacification, particularly in the right lung field. This increased opacification could be due to several reasons, including but not limited to:
 - Infiltration (e.g., pneumonia, pulmonary edema, or consolidation).
 - Mass lesion.
 - Pleural effusion.
 - Other pathologies such as fibrosis or tumor.
- The left lung field appears relatively clear compared to the right lung field.

889
890
891

Heart:

- The heart size appears to be within normal limits on this view.
- The mediastinum appears to be within normal limits.

892
893
894

Diaphragm:

- The diaphragm appears to be intact and without any obvious abnormalities.
- The costophrenic angles appear clear, which is a normal finding.

895
896
897

Bones:

- The bony structures of the thorax, including the ribs, clavicles, and scapulae, appear intact without any obvious fractures or lytic lesions.

898
899

Pleural Spaces:

- There appears to be no evidence of pleural effusion on this view.

900
901
902
903
904
905

Summary:

The X-ray shows increased opacification in the right lung field, which could be indicative of a variety of conditions. Further clinical correlation with the patient's history, symptoms, and other diagnostic tests (such as a CT scan or sputum analysis) would be necessary to determine the exact cause of the opacification. A radiologist's interpretation is recommended for a definitive diagnosis.

906
907

Recommendations:

- The patient should be evaluated by a healthcare provider for further investigation and management.
- Additional imaging or tests may be required to determine the cause of the opacification in the right lung field.

908
909

This report is for informational purposes only and should not be considered a substitute for a professional medical opinion.

910

Figure 6: MediX-R1 - Report Generation: Case 2

911
912
913
914

915 the model produced flawed reasoning despite generating the correct final answer, indicating that
916 such inconsistencies are rare and that MediX-R1 generally maintains a robust and coherent reasoning
917 process. Reviewers comprised five certified medical experts (MBBS/MD) with specialties in
918 Radiology, General Medicine, and Forensic Medicine, with an inter-rater agreement of 63%.

A.7 TRAINING DATA AND MODALITY DISTRIBUTION

We trained MediX-R1 on 51335 multimodal medical instruction samples spanning 16 modality tags. All samples were drawn from the official train splits of the source datasets: PMC-VQA subset (Zhang et al., 2024), SLAKE (Liu et al., 2021), RadVQA (Lau et al., 2018), and PathVQA (He et al., 2020).

Medical Modality	Samples
X_RAY	5964
MICROSCOPY	16399
CLINICAL_PHOTOGRAPHY	8979
CT_SCAN	7646
GRAPHICS	2205
ANGIOGRAPHY	522
PET_SCAN	406
ULTRASOUND	1227
MRI_SCAN	6224
FUNDUS_PHOTOGRAPHY	314
OCT_SCAN	236
ENDOSCOPY	611
MAMMOGRAPHY	106
FLUOROSCOPY	321
OTHER	64
SPECT	111
Total	51335

Dataset	Samples
PMC_VQA_SUBSET	25000
SLAKE	4919
RAD_VQA	1793
PATH	19623
Total	51335

Table 5: Modality Breakdown and Source Dataset composition

A.8 TRAINING CONFIGURATION

We list below the GRPO training configuration used for MediX-R1. Core settings include (i) data filtering and batching, (ii) actor optimization and rollout sampling, (iii) KL-regularized GRPO advantage computation, and (iv) trainer settings. We train our models using the EasyR1 (Zheng et al., 2025b) Github Repository. MediX-R1 was trained using 8xA100 (80 GB) Nvidia GPUs for approximately 25 hours.

Training Configuration

```
Training Configurations
"data": {
  "max_prompt_length": 4352,
  "max_response_length": 4096,
  "rollout_batch_size": 512,
  "val_batch_size": 1024,
  "shuffle": true,
  "seed": 1,
  "min_pixels": 262144,
  "max_pixels": 4194304,
  "filter_overlong_prompts": true,
  "filter_overlong_prompts_workers": 16
},
"worker": {
  "hybrid_engine": true,
  "actor": {
    "strategy": "fsdp",
    "global_batch_size": 128,
    "micro_batch_size_per_device_for_update": 1,
    "max_global_batch_size": 128
  }
}
```

```

972
973     "micro_batch_size_per_device_for_experience": 2,
974     "max_grad_norm": 1.0,
975     "clip_ratio_low": 0.2,
976     "clip_ratio_high": 0.3,
977     "clip_ratio_dual": 3.0,
978     "loss_avg_mode": "token",
979     "padding_free": true,
980     "dynamic_batching": true,
981     "use_torch_compile": true,
982     "optim": {
983         "lr": 1e-6,
984         "betas": [0.9, 0.999],
985         "weight_decay": 0.01,
986         "strategy": "adamw",
987         "lr_scheduler_type": "constant",
988         "training_steps": 200
989     },
990     "fsdp": {
991         "enable_full_shard": true,
992         "enable_rank0_init": true,
993         "mp_param_dtype": "bf16",
994         "mp_reduce_dtype": "fp32",
995         "mp_buffer_dtype": "fp32"
996     },
997     "offload": {
998         "offload_params": true,
999         "offload_optimizer": true
1000     },
1001     "use_kl_loss": true,
1002     "kl_penalty": "low_var_kl",
1003     "kl_coef": 0.01
1004 },
1005     "rollout": {
1006         "name": "vllm",
1007         "n": 5,
1008         "temperature": 1.0,
1009         "top_p": 1.0,
1010         "seed": 1,
1011         "tensor_parallel_size": 2,
1012         "max_num_batched_tokens": 8448,
1013         "gpu_memory_utilization": 0.6,
1014         "val_override_config": {
1015             "temperature": 0.6,
1016             "top_p": 0.95,
1017             "n": 1
1018         },
1019         "prompt_length": 4352,
1020         "response_length": 4096
1021     },
1022     "algorithm": {
1023         "adv_estimator": "grpo",
1024         "gamma": 1.0,
1025         "lam": 1.0,
1026         "use_kl_loss": true,
1027         "kl_penalty": "low_var_kl",
1028         "kl_coef": 0.01,
1029         "kl_type": "fixed",
1030         "kl_target": 0.1,
1031         "kl_horizon": 10000.0
1032     },
1033     "trainer": {
1034
1035
1036
1037
1038
1039
1040
1041
1042
1043
1044
1045
1046
1047
1048
1049
1050
1051
1052
1053
1054
1055
1056
1057
1058
1059
1060
1061
1062
1063
1064
1065
1066
1067
1068
1069
1070
1071
1072
1073
1074
1075
1076
1077
1078
1079
1080
1081
1082
1083
1084
1085
1086
1087
1088
1089
1090
1091
1092
1093
1094
1095
1096
1097
1098
1099
1100
1101
1102
1103
1104
1105
1106
1107
1108
1109
1110
1111
1112
1113
1114
1115
1116
1117
1118
1119
1120
1121
1122
1123
1124
1125
1126
1127
1128
1129
1130
1131
1132
1133
1134
1135
1136
1137
1138
1139
1140
1141
1142
1143
1144
1145
1146
1147
1148
1149
1150
1151
1152
1153
1154
1155
1156
1157
1158
1159
1160
1161
1162
1163
1164
1165
1166
1167
1168
1169
1170
1171
1172
1173
1174
1175
1176
1177
1178
1179
1180
1181
1182
1183
1184
1185
1186
1187
1188
1189
1190
1191
1192
1193
1194
1195
1196
1197
1198
1199
1200
1201
1202
1203
1204
1205
1206
1207
1208
1209
1210
1211
1212
1213
1214
1215
1216
1217
1218
1219
1220
1221
1222
1223
1224
1225
1226
1227
1228
1229
1230
1231
1232
1233
1234
1235
1236
1237
1238
1239
1240
1241
1242
1243
1244
1245
1246
1247
1248
1249
1250
1251
1252
1253
1254
1255
1256
1257
1258
1259
1260
1261
1262
1263
1264
1265
1266
1267
1268
1269
1270
1271
1272
1273
1274
1275
1276
1277
1278
1279
1280
1281
1282
1283
1284
1285
1286
1287
1288
1289
1290
1291
1292
1293
1294
1295
1296
1297
1298
1299
1300
1301
1302
1303
1304
1305
1306
1307
1308
1309
1310
1311
1312
1313
1314
1315
1316
1317
1318
1319
1320
1321
1322
1323
1324
1325
1326
1327
1328
1329
1330
1331
1332
1333
1334
1335
1336
1337
1338
1339
1340
1341
1342
1343
1344
1345
1346
1347
1348
1349
1350
1351
1352
1353
1354
1355
1356
1357
1358
1359
1360
1361
1362
1363
1364
1365
1366
1367
1368
1369
1370
1371
1372
1373
1374
1375
1376
1377
1378
1379
1380
1381
1382
1383
1384
1385
1386
1387
1388
1389
1390
1391
1392
1393
1394
1395
1396
1397
1398
1399
1400
1401
1402
1403
1404
1405
1406
1407
1408
1409
1410
1411
1412
1413
1414
1415
1416
1417
1418
1419
1420
1421
1422
1423
1424
1425
1426
1427
1428
1429
1430
1431
1432
1433
1434
1435
1436
1437
1438
1439
1440
1441
1442
1443
1444
1445
1446
1447
1448
1449
1450
1451
1452
1453
1454
1455
1456
1457
1458
1459
1460
1461
1462
1463
1464
1465
1466
1467
1468
1469
1470
1471
1472
1473
1474
1475
1476
1477
1478
1479
1480
1481
1482
1483
1484
1485
1486
1487
1488
1489
1490
1491
1492
1493
1494
1495
1496
1497
1498
1499
1500
1501
1502
1503
1504
1505
1506
1507
1508
1509
1510
1511
1512
1513
1514
1515
1516
1517
1518
1519
1520
1521
1522
1523
1524
1525
1526
1527
1528
1529
1530
1531
1532
1533
1534
1535
1536
1537
1538
1539
1540
1541
1542
1543
1544
1545
1546
1547
1548
1549
1550
1551
1552
1553
1554
1555
1556
1557
1558
1559
1560
1561
1562
1563
1564
1565
1566
1567
1568
1569
1570
1571
1572
1573
1574
1575
1576
1577
1578
1579
1580
1581
1582
1583
1584
1585
1586
1587
1588
1589
1590
1591
1592
1593
1594
1595
1596
1597
1598
1599
1600
1601
1602
1603
1604
1605
1606
1607
1608
1609
1610
1611
1612
1613
1614
1615
1616
1617
1618
1619
1620
1621
1622
1623
1624
1625
1626
1627
1628
1629
1630
1631
1632
1633
1634
1635
1636
1637
1638
1639
1640
1641
1642
1643
1644
1645
1646
1647
1648
1649
1650
1651
1652
1653
1654
1655
1656
1657
1658
1659
1660
1661
1662
1663
1664
1665
1666
1667
1668
1669
1670
1671
1672
1673
1674
1675
1676
1677
1678
1679
1680
1681
1682
1683
1684
1685
1686
1687
1688
1689
1690
1691
1692
1693
1694
1695
1696
1697
1698
1699
1700
1701
1702
1703
1704
1705
1706
1707
1708
1709
1710
1711
1712
1713
1714
1715
1716
1717
1718
1719
1720
1721
1722
1723
1724
1725
1726
1727
1728
1729
1730
1731
1732
1733
1734
1735
1736
1737
1738
1739
1740
1741
1742
1743
1744
1745
1746
1747
1748
1749
1750
1751
1752
1753
1754
1755
1756
1757
1758
1759
1760
1761
1762
1763
1764
1765
1766
1767
1768
1769
1770
1771
1772
1773
1774
1775
1776
1777
1778
1779
1780
1781
1782
1783
1784
1785
1786
1787
1788
1789
1790
1791
1792
1793
1794
1795
1796
1797
1798
1799
1800
1801
1802
1803
1804
1805
1806
1807
1808
1809
1810
1811
1812
1813
1814
1815
1816
1817
1818
1819
1820
1821
1822
1823
1824
1825
1826
1827
1828
1829
1830
1831
1832
1833
1834
1835
1836
1837
1838
1839
1840
1841
1842
1843
1844
1845
1846
1847
1848
1849
1850
1851
1852
1853
1854
1855
1856
1857
1858
1859
1860
1861
1862
1863
1864
1865
1866
1867
1868
1869
1870
1871
1872
1873
1874
1875
1876
1877
1878
1879
1880
1881
1882
1883
1884
1885
1886
1887
1888
1889
1890
1891
1892
1893
1894
1895
1896
1897
1898
1899
1900
1901
1902
1903
1904
1905
1906
1907
1908
1909
1910
1911
1912
1913
1914
1915
1916
1917
1918
1919
1920
1921
1922
1923
1924
1925
1926
1927
1928
1929
1930
1931
1932
1933
1934
1935
1936
1937
1938
1939
1940
1941
1942
1943
1944
1945
1946
1947
1948
1949
1950
1951
1952
1953
1954
1955
1956
1957
1958
1959
1960
1961
1962
1963
1964
1965
1966
1967
1968
1969
1970
1971
1972
1973
1974
1975
1976
1977
1978
1979
1980
1981
1982
1983
1984
1985
1986
1987
1988
1989
1990
1991
1992
1993
1994
1995
1996
1997
1998
1999
2000
2001
2002
2003
2004
2005
2006
2007
2008
2009
2010
2011
2012
2013
2014
2015
2016
2017
2018
2019
2020
2021
2022
2023
2024
2025
2026
2027
2028
2029
2030
2031
2032
2033
2034
2035
2036
2037
2038
2039
2040
2041
2042
2043
2044
2045
2046
2047
2048
2049
2050
2051
2052
2053
2054
2055
2056
2057
2058
2059
2060
2061
2062
2063
2064
2065
2066
2067
2068
2069
2070
2071
2072
2073
2074
2075
2076
2077
2078
2079
2080
2081
2082
2083
2084
2085
2086
2087
2088
2089
2090
2091
2092
2093
2094
2095
2096
2097
2098
2099
2100
2101
2102
2103
2104
2105
2106
2107
2108
2109
2110
2111
2112
2113
2114
2115
2116
2117
2118
2119
2120
2121
2122
2123
2124
2125
2126
2127
2128
2129
2130
2131
2132
2133
2134
2135
2136
2137
2138
2139
2140
2141
2142
2143
2144
2145
2146
2147
2148
2149
2150
2151
2152
2153
2154
2155
2156
2157
2158
2159
2160
2161
2162
2163
2164
2165
2166
2167
2168
2169
2170
2171
2172
2173
2174
2175
2176
2177
2178
2179
2180
2181
2182
2183
2184
2185
2186
2187
2188
2189
2190
2191
2192
2193
2194
2195
2196
2197
2198
2199
2200
2201
2202
2203
2204
2205
2206
2207
2208
2209
2210
2211
2212
2213
2214
2215
2216
2217
2218
2219
2220
2221
2222
2223
2224
2225
2226
2227
2228
2229
2230
2231
2232
2233
2234
2235
2236
2237
2238
2239
2240
2241
2242
2243
2244
2245
2246
2247
2248
2249
2250
2251
2252
2253
2254
2255
2256
2257
2258
2259
2260
2261
2262
2263
2264
2265
2266
2267
2268
2269
2270
2271
2272
2273
2274
2275
2276
2277
2278
2279
2280
2281
2282
2283
2284
2285
2286
2287
2288
2289
2290
2291
2292
2293
2294
2295
2296
2297
2298
2299
2300
2301
2302
2303
2304
2305
2306
2307
2308
2309
2310
2311
2312
2313
2314
2315
2316
2317
2318
2319
2320
2321
2322
2323
2324
2325
2326
2327
2328
2329
2330
2331
2332
2333
2334
2335
2336
2337
2338
2339
2340
2341
2342
2343
2344
2345
2346
2347
2348
2349
2350
2351
2352
2353
2354
2355
2356
2357
2358
2359
2360
2361
2362
2363
2364
2365
2366
2367
2368
2369
2370
2371
2372
2373
2374
2375
2376
2377
2378
2379
2380
2381
2382
2383
2384
2385
2386
2387
2388
2389
2390
2391
2392
2393
2394
2395
2396
2397
2398
2399
2400
2401
2402
2403
2404
2405
2406
2407
2408
2409
2410
2411
2412
2413
2414
2415
2416
2417
2418
2419
2420
2421
2422
2423
2424
2425
2426
2427
2428
2429
2430
2431
2432
2433
2434
2435
2436
2437
2438
2439
2440
2441
2442
2443
2444
2445
2446
2447
2448
2449
2450
2451
2452
2453
2454
2455
2456
2457
2458
2459
2460
2461
2462
2463
2464
2465
2466
2467
2468
2469
2470
2471
2472
2473
2474
2475
2476
2477
2478
2479
2480
2481
2482
2483
2484
2485
2486
2487
2488
2489
2490
2491
2492
2493
2494
2495
2496
2497
2498
2499
2500
2501
2502
2503
2504
2505
2506
2507
2508
2509
2510
2511
2512
2513
2514
2515
2516
2517
2518
2519
2520
2521
2522
2523
2524
2525
2526
2527
2528
2529
2530
2531
2532
2533
2534
2535
2536
2537
2538
2539
2540
2541
2542
2543
2544
2545
2546
2547
2548
2549
2550
2551
2552
2553
2554
2555
2556
2557
2558
2559
2560
2561
2562
2563
2564
2565
2566
2567
2568
2569
2570
2571
2572
2573
2574
2575
2576
2577
2578
2579
2580
2581
2582
2583
2584
2585
2586
2587
2588
2589
2590
2591
2592
2593
2594
2595
2596
2597
2598
2599
2600
2601
2602
2603
2604
2605
2606
2607
2608
2609
2610
2611
2612
2613
2614
2615
2616
2617
2618
2619
2620
2621
2622
2623
2624
2625
2626
2627
2628
2629
2630
2631
2632
2633
2634
2635
2636
2637
2638
2639
2640
2641
2642
2643
2644
2645
2646
2647
2648
2649
2650
2651
2652
2653
2654
2655
2656
2657
2658
2659
2660
2661
2662
2663
2664
2665
2666
2667
2668
2669
2670
2671
2672
2673
2674
2675
2676
2677
2678
2679
2680
2681
2682
2683
2684
2685
2686
2687
2688
2689
2690
2691
2692
2693
2694
2695
2696
2697
2698
2699
2700
2701
2702
2703
2704
2705
2706
2707
2708
2709
2710
2711
2712
2713
2714
2715
2716
2717
2718
2719
2720
2721
2722
2723
2724
2725
2726
2727
2728
2729
2730
2731
2732
2733
2734
2735
2736
2737
2738
2739
2740
2741
2742
2743
2744
2745
2746
2747
2748
2749
2750
2751
2752
2753
2754
2755
2756
2757
2758
2759
2760
2761
2762
2763
2764
2765
2766
2767
2768
2769
2770
2771
2772
2773
2774
2775
2776
2777
2778
2779
2780
2781
2782
2783
2784
2785
2786
2787
2788
2789
2790
2791
2792
2793
2794
2795
2796
2797
2798
2799
2800
2801
2802
2803
2804
2805
2806
2807
2808
2809
2810
2811
2812
2813
2814
2815
2816
2817
2818
2819
2820
2821
2822
2823
2824
2825
2826
2827
2828
2829
2830
2831
2832
2833
2834
2835
2836
2837
2838
2839
2840
2841
2842
2843
2844
2845
2846
2847
2848
2849
2850
2851
2852
2853
2854
2855
2856
2857
2858
2859
2860
2861
2862
2863
2864
2865
2866
2867
2868
2869
2870
2871
2872
2873
2874
2875
2876
2877
2878
2879
2880
2881
2882
2883
2884
2885
2886
2887
2888
2889
2890
2891
2892
2893
2894
2895
2896
2897
2898
2899
2900
2901
2902
2903
2904
2905
2906
2907
2908
2909
2910
2911
2912
2913
2914
2915
2916
2917
2918
2919
2920
2921
2922
2923
2924
2925
2926
2927
2928
2929
2930
2931
2932
2933
2934
2935
2936
2937
2938
2939
2940
2941
2942
2943
2944
2945
2946
2947
2948
2949
2950
2951
2952
2953
2954
2955
2956
2957
2958
2959
2960
2961
2962
2963
2964
2965
2966
2967
2968
2969
2970
2971
2972
2973
2974
2975
2976
2977
2978
2979
2980
2981
2982
2983
2984
2985
2986
2987
2988
2989
2990
2991
2992
2993
2994
2995
2996
2997
2998
2999
3000
3001
3002
3003
3004
3005
3006
3007
3008
3009
3010
3011
3012
3013
3014
3015
3016
3017
3018
3019
3020
3021
3022
3023
3024
3025
3026
3027
3028
3029
3030
3031
3032
3033
3034
3035
3036
3037
3038
3039
3040
3041
3042
3043
3044
3045
3046
3047
3048
3049
3050
3051
3052
3053
3054
3055
3056
3057
3058
3059
3060
3061
3062
3063
3064
3065
3066
3067
3068
3069
3070
3071
3072
3073
3074
3075
3076
3077
3078
3079
3080
3081
3082
3083
3084
3085
3086
3087
3088
3089
3090
3091
3092
3093
3094
3095
3096
3097
3098
3099
3100
3101
3102
3103
3104
3105
3106
3107
3108
3109
3110
3111
3112
3113
3114
3115
3116
3117
3118
3119
3120
3121
3122
3123
3124
3125
3126
3127
3128
3129
3130
3131
3132
3133
3134
3135
3136
3137
3138
3139
3140
3141
3142
3143
3144
3145
3146
3147
3148
31
```

```
1026
1027     "total_epochs": 2,
1028     "nnodes": 1,
1029     "n_gpus_per_node": 8,
1030     "val_freq": 5,
1031     "val_before_train": true,
1032     "save_freq": 5,
1033     "save_limit": 3
1034 }
```

A.9 REWARD FUNCTION SOURCE CODE

1038 Below are the Python implementations of the four reward components used in MediX-R1. Each
1039 function operates on a predicted model output string and a ground truth string containing the modal-
1040 ity tag and reference answer.

Format reward

```
1044 def format_reward(predict: str) -> float:
1045     idx = predict.find("<think>")
1046     if idx == -1:
1047         return 0.0
1048     predict_new = predict[idx:].strip()
1049     pattern = re.compile(r"<think>.*?</think>\s*<answer>.*?</answer>",
1050                          re.DOTALL)
1051     format_match = re.fullmatch(pattern, predict_new)
1052     return 1.0 if format_match else 0.0
```

LLM-based accuracy reward

```
1056 def accuracy_reward_llm(predict: str, ground_truth: str) -> float:
1057     try:
1058         content_match = re.search(r"<answer>(.*)</answer>", predict,
1059                                     re.DOTALL)
1060         given_answer = content_match.group(1).strip() if content_match
1061             else predict.strip()
1062         given_answer = given_answer.strip('.')
1063         ground_truth = ground_truth.split('>', maxsplit=1)[1].strip()
1064         ground_truth = ground_truth.strip('.')
1065
1066         if given_answer == '' or len(given_answer) == 1:
1067             return 0.0
1068         if given_answer == ground_truth:
1069             return 1.0
1070         llm_score = llm_answer_match(given_answer, ground_truth) #
1071             external helper
1072         return llm_score
1073     except Exception:
1074         return 0.0
```

Embedding-based semantic reward

```
1077     def accuracy_reward_embed(predict: str, ground_truth: str, threshold
1078         : float = 0.8) -> float:
1079         try:
```

```

1080
1081     content_match = re.search(r"<answer>(.*)</answer>", predict,
1082                             re.DOTALL)
1083     given_answer = content_match.group(1).strip() if content_match
1084     else predict.strip()
1085     given_answer = given_answer.strip('.')
1086     ground_truth = ground_truth.split('>', maxsplit=1)[1].strip()
1087     ground_truth = ground_truth.strip('.')
1088
1088     if given_answer == '' or len(given_answer) == 1:
1089         return 0.0
1090     if given_answer == ground_truth:
1091         return 1.0
1092
1092     embeddings = embed_model.encode([given_answer, ground_truth],
1093                                     convert_to_tensor=True)
1094     similarity = util.pytorch_cos_sim(embeddings[0], embeddings
1095                                         [1]).item()
1095     return float(similarity >= threshold)
1096 except Exception:
1097     return 0.0
1098
1099

```

Modality recognition reward

```

1100
1101
1102 def modality_reward(predict: str, ground_truth: str) -> float:
1103     idx = predict.find("<think>")
1104     if idx == -1:
1105         return 0.0
1106     predict_new = predict[:idx].strip() # modality tag before <think>
1107     modality = ground_truth.split('>', maxsplit=1)[0] + '>'
1108     return 1.0 if predict_new.upper() == modality.upper() else 0.0
1109
1110

```

A.10 EVALUATION ON REAL WORLD CLINICAL DATA

To further assess the generalization ability of our model, we conducted additional evaluation on MedPix 2.0 (Siragusa et al., 2025), a publicly available real-world clinical VQA dataset derived from the original MedPix (Henigman & Kennedy, 2025) database maintained by the U.S. National Library of Medicine (NIH). MedPix comprises over 12,000 anonymized, crowdsourced clinical cases containing medical images and corresponding textual information such as findings, diagnoses, and treatments. This ensures both reproducibility and compliance with NIH privacy standards.

The evaluation on MedPix 2.0 demonstrates that our model, MediX-R1, consistently outperforms other medical vision-language models. Specifically, MediX-R1 achieves a score of 51.11%, surpassing strong baselines and previous SOTA Medical Models as shown in Table 6. These results further confirm the robustness and adaptability of MediX-R1 on diverse real-world clinical data, emphasizing its capability to generalize beyond controlled experimental environments.

Model	Score (%)
MedVLM-R1	27.57
MedGemma	43.18
LLaVA-Med	44.29
BiMediX2	46.51
HuatuoGPT	48.81
MediX-R1 (Ours)	51.11

Table 6: Performance comparison on the MedPix 2.0 dataset.